ORGANIC CHEMISTRY FRONTIERS

RESEARCH ARTICLE

View Article Online
View Journal | View Issue

Cite this: *Org. Chem. Front.*, 2020, **7**, 2047

DFT study on the *E*-stereoselective reductive A^3-coupling reaction of terminal alkynes with aldehydes and 3-pyrroline†

Yuan Yao,[a] Xue Zhang *[b] and Shengming Ma *[a,b]

Received 21st May 2020,
Accepted 22nd June 2020

DOI: 10.1039/d0qo00564a

rsc.li/frontiers-organic

The mechanism of the Cu(I)-catalyzed reductive A^3-coupling reaction of terminal alkynes with aldehydes and 3-pyrroline for the synthesis of *E*-allylic amines has been studied by DFT calculations. The calculations suggest that the pathway selectivity is determined by the activation energy difference between β-N elimination and protodemetalation from the iminium intermediate (**INT7**) formed *via* the rate-limiting 1,5-H transfer of the CuBr-coordinated propargylic amine (**INT4**). The stepwise intermolecular protodemetalation assisted by 3-pyrroline or water cluster proceeds more efficiently than β-N elimination, resulting in the formation of an allylic amine instead of an allene as the final product. Notably, the aromatization of the azacycle (formed from 3-pyrroline) is an essential driving force for the preference of the allylic amine products. In addition, the formation of a hydrogen bond between the hydroxyl group of the terminal alkyne and the migrating hydrogen stabilizes the transition state of the 1,5-H transfer step, thus, increasing the reaction reactivity.

Introduction

Metal-catalyzed three-component coupling of an alkyne, an aldehyde and an amine (A^3-coupling) is a straightforward protocol for preparing propargylic amines,[1] which serve as the key intermediates for the synthesis of many organic compounds.[2] Mechanistically, the A^3-coupling involves the reaction of the *in situ* generated metal alkynylide species **A** with the iminium ion **B** that is *in situ* generated from the condensation of an aldehyde with an amine, resulting in the formation of the metal-coordinated propargylic amine **C**, which undergoes 1,5-H transfer to afford the iminium intermediate **D** (Scheme 1). Subsequent β-N elimination would produce the allene product (path a in Scheme 1).[3] This mechanism has been supported by our detailed theoretical studies.[3c] It is worth noting that the amine in these reactions can be diisopropylamine,[2f] dicyclohexylamine,[2g] morpholine,[2h] pyrrolidine,[2i,k,n] diphenylprolinol,[2j,m] tetrahydroisoquinoline,[2l] azocane,[2o] and so on. Interestingly, *E*-allylic amines were obtained unexpectedly when terminal alkynes and aldehydes were treated with 3-pyrroline or isoindoline in the presence of copper(I) (path b in Scheme 1).[4] We presumed that the *E*-allylic amine is afforded through the protodemetalation process after the generation of the iminium intermediate **D**. Deuterium-labeling experiments have been performed to confirm that the β-position proton of *E*-allylic amines came from the azacycle and the α-position proton came from the proton in the ambient environment (Scheme 2).[4] Here, we sought to investi-

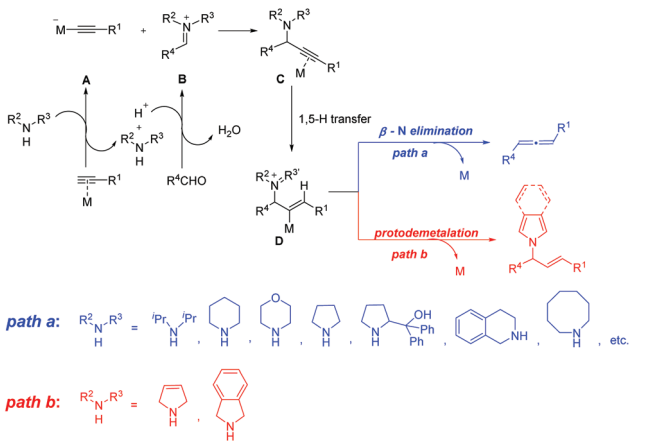

Scheme 1 (a) A general mechanism for the metal-catalyzed A^3-coupling reaction followed by 1,5-H transfer and β-N elimination affording an allene (ATA reaction). (b) Reductive A^3-coupling for the synthesis of *E*-allylic amines.

[a]*Research Center for Molecular Recognition and Synthesis, Department of Chemistry, Fudan University, 220 Handan Lu, Shanghai 200433, P. R. China*
[b]*State Key Laboratory of Organometallic Chemistry, Shanghai Institute of Organic Chemistry, Chinese Academy of Sciences, 345 Lingling Lu, Shanghai 200032, P. R. China. E-mail: xzhang@sioc.ac.cn, masm@sioc.ac.cn*

†Electronic supplementary information (ESI) available. See DOI: 10.1039/d0qo00564a

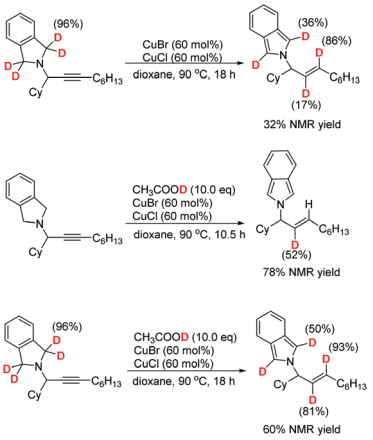

Scheme 2 Deuterium-labeling experiments.

gate the detailed reaction mechanism of this Cu(I)-catalyzed[5] reductive A^3-coupling reaction, as well as the crucial role of 3-pyrroline or isoindoline. The origin of the different chemoselectivity of the afforded allylic amine or allene was also discussed.

Computational methods

DFT calculations were carried out using the Gaussian 09 software.[6] M06-2X,[7] including Grimme's D3 dispersion corrections, was employed to performed geometry optimizations. The LANL2DZ[8] basis set in conjunction with the LANL2DZ pseudopotential[9] was used for Cu and Br atoms, while the 6-31G(d,p)[10] basis set was used for the other atoms. Geometry optimizations were fully carried out. Harmonic vibration frequency calculations were conducted at the same level of theory to verify the stationary points to be the minima (no imaginary frequency) or saddle points (one imaginary frequency). Intrinsic reaction coordinate (IRC)[11] calculations were performed to confirm the connection of the transition structures with their corresponding reactants and products. The single point energies and solvent effects in toluene (ε = 2.37) were computed with M06-2X-D3/SDD[12]-6-311++G(d,p) basis sets by using the SMD[13] solvation model. The solution-phase Gibbs free energy was used in the present discussions. The calculations were carried out on the exact compounds applied experimentally: 2-methybut-3-yn-2-ol (**1**), cyclohexanaldehyde (**2**) and 3-pyrroline (**3**) with copper(I) bromide as the catalyst (Scheme 3).

Scheme 3

Results and discussion

The A^3-coupling reaction proceeds initially from the sp C–H activation of the terminal alkyne **1** by the metal catalyst and the condensation of cyclohexanaldehyde **2** with 3-pyrroline **3**, affording the ion pair **Int3**, which consists of copper alkynylide anion **Int1** and iminium cation **Int2**. This process leads to an energy increase of 4.0 kcal mol^{-1}, accompanied by the loss of one molecule of water. The subsequent electrophilic attack of iminium **Int2** on the copper attached C^1 *via* **TS1** requires an energy barrier of 10.1 kcal mol^{-1}, providing the propargyl amine–CuBr complex **Int4**. Subsequent isomerization of **Int4** to **Int5**, affording the precursor for 1,5-H transfer, in which CuBr and the amino group are in the *trans* position, is endergonic by 7.4 kcal mol^{-1} relative to **Int4**.

With the envelope conformation of the pyrrolidine moiety in **Int5**, there are two axial hydrogen atoms (H^1 and H^2 in Fig. 1) in perfect orientation for transfer to the C^2 atom. The six-membered cyclic transition state for the 1,5-H transfer has been located as **TS2_1** and **TS2_2** for the transfer of H^1 and H^2 atoms, respectively. The free energy barrier for 1,5-H^1 transfer is calculated to be 27.7 kcal mol^{-1} (**TS2_1** relative to **Int4**), which is lower by 1.8 kcal mol^{-1} than that for the 1,5-H^2 transfer (**TS2_2**), due to the fact that H^1 is closer than H^2 to the C^2 atom (2.80 Å *vs.* 3.03 Å). Hence, **TS2_1** is more favorable, leading to the formation of *N*-allylic iminium–CuBr intermediate **Int6_1**, during which a σ bond between Cu(I) and C1 is formed. Subsequent isomerization of **Int6_1** by single-bond rotation produces the more stable species **Int7**, which is exergonic by 3.6 kcal mol^{-1} relative to **Int6_1**. The 1,5-H transfer step features the highest free energy barrier of the whole profile (27.7 kcal mol^{-1}, **TS2_1**), and may, thus, be rate determining.

From iminium intermediate **Int7**, there are two alternative pathways: one is β-N elimination to produce the allene product (path a in Fig. 2), and the other is the protodemetalation process to afford the allylic amine (path b in Fig. 2). The optimized transition structure for path a has been located as **TS3** and **TS4**, in which the C–N and C–Cu bonds break simultaneously. The *cis* elimination from **Int7** proceeds through **TS3**, which requires an energy barrier of 24.9 kcal mol^{-1} (**TS3** relative to **Int7**). However, the *trans* elimination through **TS4** is much easier with a barrier of 14.3 kcal mol^{-1}. The precursor for **TS4** is **Int8**, which is provided through the single-bond rotation of **Int7**. Thus, we consider that the β-N elimination should be in a *trans* manner through **TS4**, which needs to overcome a free energy barrier of 14.3 kcal mol^{-1} to afford **Int9**. Finally, allene **5** is released from **Int9**, with an overall exergonicity of 19.2 kcal mol^{-1} (relative to **Int7**).

An alternative pathway from allyl iminium–CuBr intermediate **Int7** is the protodemetalation process to afford the allylic amine (path b in Fig. 2), which is the only product obtained experimentally. The direct intramolecular protodemetalation of **Int7** proceeds through a concerted five-membered cyclic transition structure (**TS5**), in which the deprotonation of the alkyl hydrogen (H^3) adjacent to the N atom and

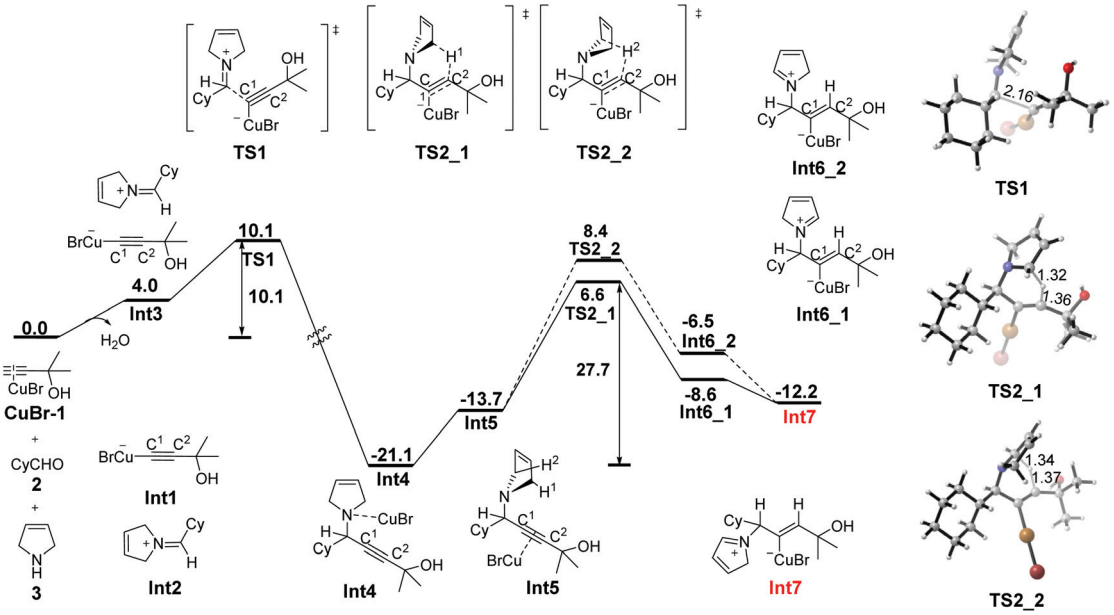

Fig. 1 Free energy profile (ΔG in kcal mol^{-1}) for the formation of the propargylic amine and the subsequent 1,5-H transfer. Bond lengths are given in angstroms.

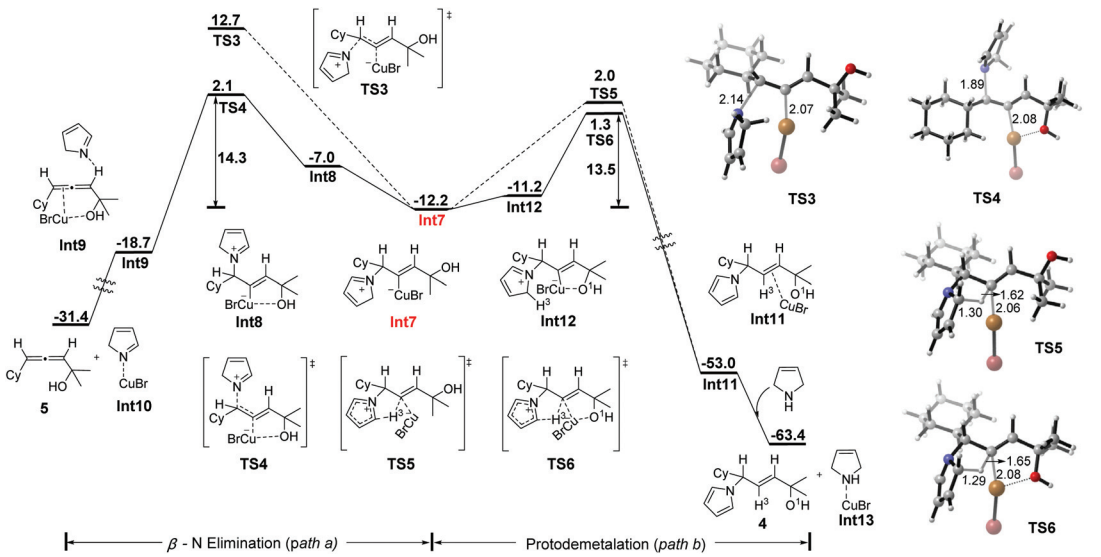

Fig. 2 Free energy profile (ΔG in kcal mol^{-1}) for either intramolecular protodemetalation or β-N elimination from **Int7**. Bond lengths are given in angstroms.

protodemetalation of CuBr take place simultaneously, leading to the CuBr-coordinated allylic amine **Int11**. This process is computed to be exergonic (ΔG = −40.8 kcal mol^{-1}) and requires a 14.2 kcal mol^{-1} activation barrier (**TS5** relative to **Int7**). However, **Int7** can isomerize to a less stable species **Int12** (1.0 kcal mol^{-1} higher in energy than **Int7**) through single-bond rotation with the hydroxyl group coordinating to the Cu atom (d(Cu···O) = 2.41 Å). **Int12** may serve as the precursor for the protodemetalation process as well, which also proceeds through a concerted five-membered cyclic transition structure (**TS6**). **TS6** needs to overcome a free energy barrier of 13.5 kcal mol^{-1}, which is lower in energy by 0.7 kcal mol^{-1} than **TS5** (14.2 kcal mol^{-1}), leading to **Int11** as well. Thus, we consider that **TS6** is preferable to **TS5** for the direct intramolecular protodemetalation of **Int7**. The final step of this process involves the release of the product allylic amine **4** through CuBr coordinated to another 3-pyrroline molecule, which is calculated to be exergonic by 10.4 kcal mol^{-1} (relative to **Int11**) due to the strong coordination ability of nitrogen with CuBr.

The abovementioned computational results show that the direct protodemetalation is preferred over β-N elimination both kinetically and thermodynamically, indicating that an allylic amine should be obtained as the major product. However, in the experiment, allylic amines are obtained as the only products, and allenes are not observed at all. We do not think that the free energy difference of 0.8 kcal mol^{-1} could account for the exclusive formation of allylic amines. In addition, deuterium-labeling experiments confirm that the β-position proton of allylic amines may come from not only the azacycle but also the moisture in the ambient environment (Scheme 2).[4] Hence, the stepwise protodemetalation assisted by other molecules is taken into account. When one molecule of water is taken into consideration,[14] the single bond C^2–C^3 in **Int7** rotates to facilitate the hydrogen bond formation between the hydroxyl group and the H^4 in water, leading to the formation of the complex **Int14**, in which three hydrogen bonds take shape with water [$d(O^2\cdots H^3)$ = 2.23 Å, $d(O^1\cdots H^4)$ = 1.96 Å, $d(Br\cdots H^5)$ = 2.73 Å] (Fig. 3). The deprotonation process of **Int14** involves the abstraction of the proton H^3 from the azacycle by water and the subsequent protonation of the hydroxyl group, affording the intermediate **Int15**, in which the protonated hydroxyl group is stabilized by the hydrogen bond formed with water. This deprotonation process, accompanied by the aromatization of the azacycle of **Int14**, requires a free energy barrier of 8.1 kcal mol^{-1} (**TS7**, relative to **Int7**). Isomerization of **Int15** to **Int16** facilitates the subsequent protodemetalation process, which takes place intramolecularly through a concerted five-membered cyclic transition state (**TS8**). **TS8** is calculated to be higher in electronic energy by only 1.8 kcal mol^{-1} than **Int16**. However, when the thermal correction and the solvent effect are taken into account, **TS8** is slightly lower in free energy than intermediate **Int16**, indicating that the water-assisted protodemetalation could proceed with almost no barrier to afford the CuBr-coordinated allylic amine **Int17**. Finally, the product allylic amine **4** can be obtained by the coordination of CuBr to another 3-pyrroline molecule.

When the water cluster, modeled by three molecules of water, is taken into account, a similar energy profile is obtained, which is shown in Fig. 4. The water cluster assisted deprotonation requires to overcome a lower energy barrier of 5.2 kcal mol^{-1}. Different from the one water molecule assisted pathway, the subsequent protodemetalation takes place in an intermolecular way with an energy barrier of 4.2 kcal mol^{-1}.

Calculations show that the presence of water (or water cluster) turns the direct concerted protodemetalation into a reversible stepwise deprotonation–protodemetalation process, which requires a much lower free energy barrier in total. Obviously, water (or the water cluster) may act as a proton shuttle in this process, making the protodemetalation process more kinetically favorable.

Interestingly, when an additional 3-pyrroline was taken into account as the proton shuttle, another kinetically favorable pathway of the stepwise deprotonation–protodemetalation process was discovered (Fig. 5). All efforts to locate the hydrogen-bonding complex of 3-pyrroline with **Int7** were unsuccessful. When the N atom of 3-pyrroline approaches the proton H^3 of the azacycle of **Int7**, the abstraction of H^3 takes place immediately, indicating that the deprotonation process of **Int7** requires no barrier in the presence of 3-pyrroline. The abstraction of the proton H^3 from **Int7** produces **Int21**, which is exergonic by 24.5 kcal mol^{-1}, accompanied by the aromatization of the azacycle. The subsequent protodemetalation takes place intermolecularly by the protonated 3-pyrroline through **TS11** with an energy barrier of 2.3 kcal mol^{-1}, affording the more stable CuBr-coordinated allyl amine **Int22**. Finally, the coordination of CuBr with 3-pyrroline releases allylic amine **4** to com-

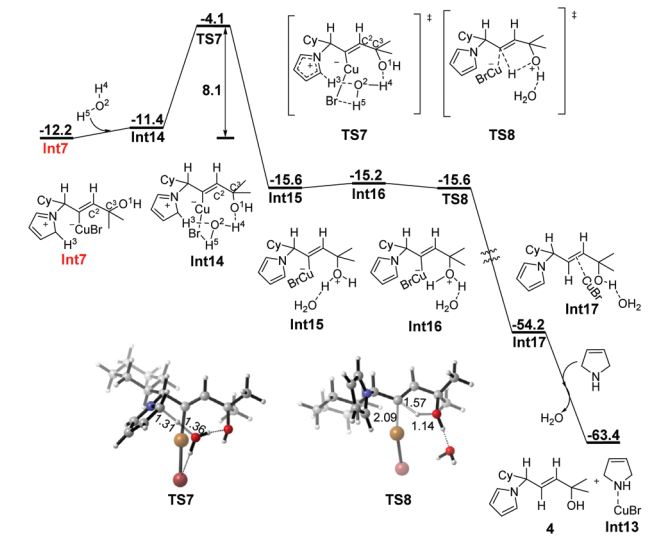

Fig. 3 Free energy profile (ΔG in kcal mol^{-1}) for H_2O-assisted stepwise protodemetalation of **Int7**. Bond lengths are given in angstroms.

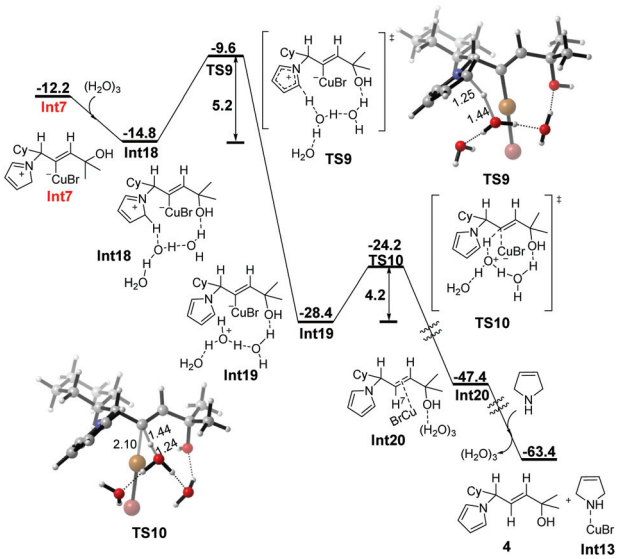

Fig. 4 Free energy profile (ΔG in kcal mol^{-1}) for water cluster-assisted stepwise protodemetalation of **Int7**. Bond lengths are given in angstroms.

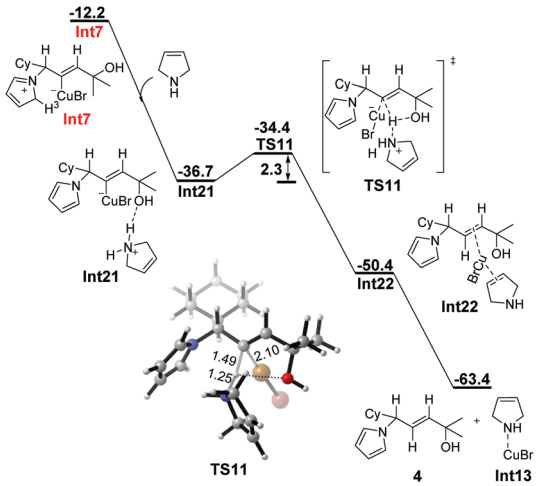

Fig. 5 Free energy profile (Δ*G* in kcal mol^{-1}) for 3-pyrroline-assisted stepwise protodemetalation of **Int7**. Bond lengths are given in angstroms.

plete the whole process. Thus, an extra 3-pyrroline molecule could also act as the proton shuttle to change the concerted protodemetalation process to a stepwise deprotonation–protodemetalation process. But different from the water (or water cluster) involved pathway, the rate-limiting step of the 3-pyrroline assisted process is the protodemetalation step with an activation barrier of only 2.3 kcal mol^{-1}.

The propargylic alcohol **1**, as one of the reactants, may also act as a proton shuttle to assist the protodemetalation process (Fig. 6). The computed potential energy surface is qualitatively similar to that of the one water molecule assisted pathway, but with more energy demanded in the deprotonation step, which needs to overcome an activation barrier of 10.1 kcal mol^{-1} (**TS12**). The following protodemetalation proceeds intramolecularly with an energy barrier of 1.8 kcal mol^{-1}.

The normal terminal alkynes with no hydroxy group present relatively lower reactivities in the experimental studies.[4] For example, when using 1-octyne under the standard reaction conditions, the *E*-allylic amine was also formed with a lower yield (20% NMR yield), accompanied by 70% NMR yield of the propargylic amine.[4] The effect of the hydroxyl group in 2-methybut-3-yn-2-ol (**1**) was further rationalized by DFT calculations on comparison with the 1-octyne-participated system.[15] The computed potential energy surfaces are qualitatively similar to those of the 2-methybut-3-yn-2-ol (**1**)-involved system, but with more free energy demanded in the rate-limiting 1,5-H transfer step [28.8 kcal mol^{-1} (**TS15_1**) *vs.* 27.7 (**TS2_1**)], which is in accordance with the experimental observations. As shown in Fig. 7, the hydrogen bond, formed

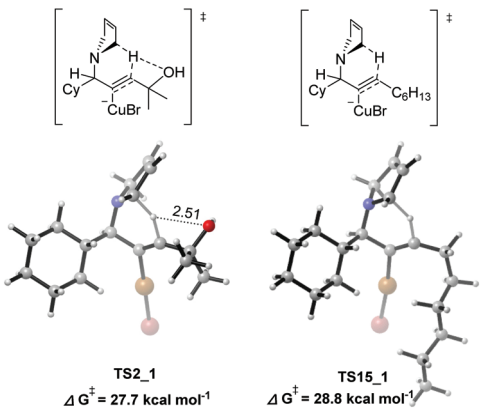

Fig. 7 Optimized transition structures for 1,5-H transfer. Bond lengths are given in angstroms.

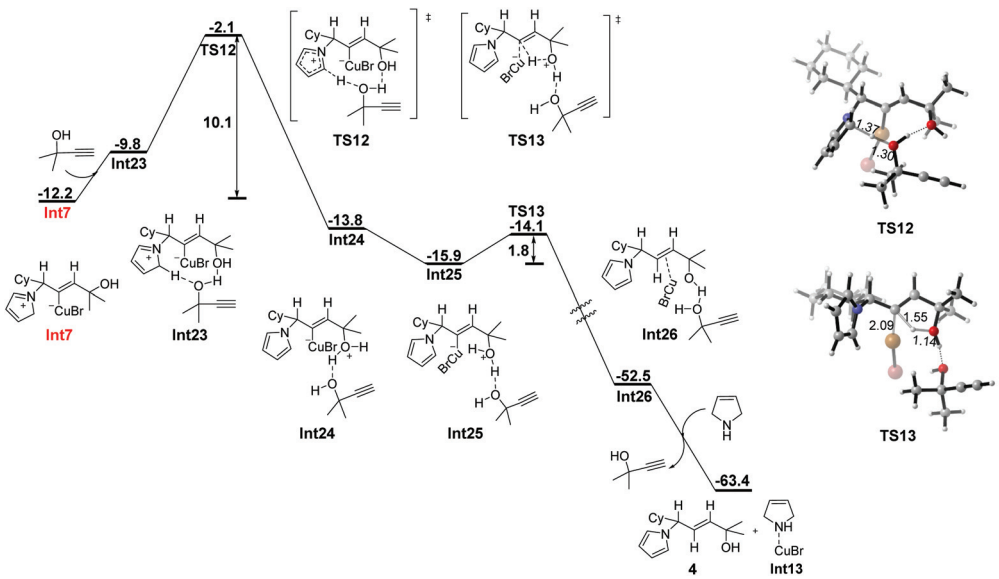

Fig. 6 Free energy profile (Δ*G* in kcal mol^{-1}) for propargylic alcohol-assisted stepwise protodemetalation of **Int7**. Bond lengths are given in angstroms.

Table 1 Activation energies (ΔG in kcal mol^{-1}) for the processes from **Int7**

Protodemetalation							
Assisting species	None[a]	H_2O	$(H_2O)_3$			β-N Elimination	
Deprotonation	13.5	8.1	5.2	No barrier	10.1	14.3	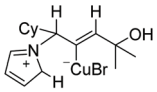
Protodemetalation		No barrier	4.2	2.3	1.8		

Int7

[a] The protodemetalation proceeds in a concerted manner.

between the hydroxyl group and the migrating hydrogen [d(O···H) = 2.51 Å] in **TS2_1**, facilitates the 1,5-H transfer, resulting in the enhanced stability of **TS2_1**.

Conclusions

The activation energies for the stepwise deprotonation–protodemetalation process of **Int7** assisted by different species are presented separately in Table 1, together with the energy barrier of the β-N elimination process. It is obvious that the direct intramolecular pathway without the aid of other species is unfavorable, owing to the high energy demand of 13.5 kcal mol^{-1}. The presence of different assisting species makes the concerted intramolecular process an irreversible stepwise deprotonation–protodemetalation process, reducing the activation barrier significantly. Among the four assisting species, 3-pyrroline shows the highest activity in the deprotonation step owing to the relatively strong basicity of the N atom. Once the rate-limiting 1,5-H transfer completes, the deprotonation–protodemetalation process takes place immediately with the aid of 3-pyrroline to afford the final allylic amine product. It is noteworthy that without 3-pyrroline (or isoindoline) in the reaction system, other species, such as water cluster, could also act as the proton shuttle to assist the protodemetalation, which is in agreement with the observation in deuterium-labeling experiments (Scheme 2). Significantly, the aromatization of the azacycle is the essential driving force for the protodemetalation process.

The pathway selectivity is determined by the activation energy difference between β-N elimination and the protodemetalation from the intermediate **Int7** formed *via* the 1,5-H transfer. Consistent with the experimental observations, with 3-pyrroline, protodemetalation is favored over β-N elimination by 12.0 kcal mol^{-1} (14.3 kcal mol^{-1} *vs.* 2.3 kcal mol^{-1}), leading to the overwhelming formation of the allylic amine product. However, all the other amines listed in Scheme 1, other than 3-pyrroline and isoindoline, completely reverse the pathway selectivity, providing allenes as the final products. Due to the lack of the driving force arising from the aromatization of the azacycle, the protodemetalation of the intermediate **D** (Scheme 1) is rather difficult. Therefore, β-N elimination becomes the favorable pathway for the classical ATA reactions using the amines except 3-pyrroline or isoindoline.

In summary, the mechanism of this Cu(I)-catalyzed reductive A^3-coupling reaction affording *E*-allylic amines was investigated by DFT calculations in detail. The calculations disclose that 3-pyrroline (or isoindoline) serves not only as a reactant but also as a shuttle in a proton relay to assist the protodemetalation step, resulting in the production of an allylic amine other than an allene. Importantly, the calculations reveal the factors governing the selectivity: the aromatization of the azacycle (formed from 3-pyrroline or isoindoline) is the essential driving force for the preference of the allylic amine products. Furthermore, we also discovered that formation of a hydrogen bond with the migrating hydrogen to facilitate the rate-determining 1,5-H transfer step is the key role of the hydroxyl group in the terminal alkyne substrate in the reactivity.

Conflicts of interest

There are no conflicts to declare.

Acknowledgements

Financial support from the Natural Science Foundation of Shanghai (19ZR1468500) and the National Natural Science Foundation of China (Grant No. 21690063 for S. Ma) is greatly appreciated.

Notes and references

1 For selected reviews on the synthesis of propargylic amines, see: (*a*) C. Wei, Z. Li and C.-J. Li, The development of A^3-coupling (Aldehyde-Alkyne-Amine) and AA^3-coupling (Asymmetric Aldehyde-Alkyne-Amine), *Synlett*, 2004, 1472; (*b*) L. Zani and C. Bolm, Direct addition of alkynes to imines and related C=N electrophiles: a convenient access to propargylamines, *Chem. Commun.*, 2006, 4263; (*c*) W.-J. Yoo, L. Zhao and C.-J. Li, The A^3-coupling (Aldehyde-Alkyne-Amine) reaction: a versatile method for the preparation of propargylamines, *Aldrichimica Acta*,

2011, **44**, 43; (*d*) V. A. Peshkov, O. P. Pereshivko and E. V. Van der Eycken, A walk around the A^3-coupling, *Chem. Soc. Rev.*, 2012, **41**, 3790.

2 For selected reviews on the synthesis of allenes through propargylic amines, see: (*a*) R. K. Neff and D. E. Frantz, Recent advances in the catalytic syntheses of allenes: a critical assessment, *ACS Catal.*, 2014, **4**, 519; (*b*) J. Ye and S. Ma, Conquering three-carbon axial chirality of allenes, *Org. Chem. Front.*, 2014, **1**, 1210; (*c*) X. Huang and S. Ma, Allenation of terminal alkynes with aldehydes and ketones, *Acc. Chem. Res.*, 2019, **52**, 1301. For selected examples of the synthesis of allenes through propargylic amines, see: (*d*) V. K.-Y. Lo, M.-K. Wong and C.-M. Che, Gold-catalyzed highly enantioselective synthesis of axially chiral allenes, *Org. Lett.*, 2008, **10**, 517; (*e*) V. K.-Y. Lo, C.-Y. Zhou, M.-K. Wong and C.-M. Che, Silver(I)-mediated highly enantioselective synthesis of axially chiral allenes under thermal and microwave-assisted conditions, *Chem. Commun.*, 2010, **46**, 213; (*f*) P. Crabbé, H. Fillion, D. André and J.-L. Luche, Efficient homologation of acetylenes to allenes, *J. Chem. Soc., Chem. Commun.*, 1979, 859; (*g*) J. Kuang and S. Ma, An efficient synthesis of terminal allenes from terminal 1-alkynes, *J. Org. Chem.*, 2009, **74**, 1763; (*h*) J. Kuang and S. Ma, One-pot synthesis of 1,3-disubstituted allenes from 1-alkynes, aldehydes, and morpholine, *J. Am. Chem. Soc.*, 2010, **132**, 1786; (*i*) J. Ye, S. Li, B. Chen, W. Fan, J. Kuang, J. Liu, Y. Liu, B. Miao, B. Wan, Y. Wang, X. Xie, Q. Yu, W. Yuan and S. Ma, Catalytic asymmetric synthesis of optically active allenes from terminal alkynes, *Org. Lett.*, 2012, **14**, 1346; (*j*) J. Ye, W. Fan and S. Ma, *tert*-Butyldimethylsilyl-directed highly enantioselective approach to axially chiral α-allenols, *Chem. – Eur. J.*, 2013, **19**, 716; (*k*) X. Tang, C. Zhu, T. Cao, J. Kuang, W. Lin, S. Ni, J. Zhang and S. Ma, Cadmium iodide-mediated allenylation of terminal alkynes with ketones, *Nat. Commmun.*, 2013, **4**, 2450; (*l*) G.-J. Jiang, Q.-H. Zheng, M. Dou, L.-G. Zhuo, W. Meng and Z.-X. Yu, Mild-condition synthesis of allenes from alkynes and aldehydes mediated by tetrahydroisoquinoline (THIQ), *J. Org. Chem.*, 2013, **78**, 11783; (*m*) X. Huang, T. Cao, Y. Han, X. Jiang, W. Lin, J. Zhang and S. Ma, General $CuBr_2$-catalyzed highly enantioselective approach for optically active allenols from terminal alkynols, *Chem. Commun.*, 2015, **51**, 6956; (*n*) Q. Liu, X. Tang, Y. Cai and S. Ma, Catalytic one-pot synthesis of trisubstituted allenes from terminal alkynes and ketones, *Org. Lett.*, 2017, **19**, 5174; (*o*) Q. Liu, T. Cao, Y. Han, X. Jiang, Y. Tang, Y. Zhai and S. Ma, Copper(I) iodide-catalyzed asymmetric synthesis of optically active tertiary α-allenols, *Synlett*, 2019, **30**, 477.

3 For computational investigations on the synthesis of allenes through 1,5-H transfer and β-elimination, see: (*a*) C. Liao, B. Li, J. Wang and Y. Wang, Mechanism of silver(I)-catalyzed enantioselective synthesis of axially chiral allenes based on propargylamines, *Chin. J. Chem.*, 2012, **30**, 951; (*b*) M. González, R. Á. Rodríguez, M. M. Cid and C. S. López, A stepwise retro-imino-ene as a key step in the mechanism of allene formation via the Crabbé acetylene homologation, *J. Comput. Chem.*, 2012, **33**, 1236; (*c*) X. Zhang, A computational study of allene synthesis via the ZnI_2-promoted allylation of terminal alkynes (ATA reaction), *Asian J. Org. Chem.*, 2014, **3**, 309; (*d*) Y. Han and X. Zhang, Theoretical studies of allene synthesis through cadmium iodide-mediated allenylation of terminal alkynes, *Asian J. Org. Chem.*, 2017, **6**, 1778.

4 W. Fan, W. Yuan and S. Ma, Unexpected *E*-stereoselective reductive A^3-coupling reaction of terminal alkynes with aldehydes and amines, *Nat. Commun.*, 2014, **5**, 3884.

5 For selected examples involving DFT calculations on Cu-catalyzed or Cu-mediated reactions, see ref. 3*b* and: (*a*) K. Zhong, C. Shan, L. Zhu, S. Liu, T. Zhang, F. Liu, B. Shen, Y. Lan and R. Bai, Theoretical study of the addition of Cu–carbenes to acetylenes to form chiral allenes, *J. Am. Chem. Soc.*, 2019, **141**, 5772; (*b*) S.-J. Li and Y. Lan, Is Cu(III) a necessary intermediate in Cu-mediated coupling reactions? a mechanistic point of view, *Chem. Commun.*, 2020, **56**, 6609; (*c*) S. Liu, H. Liu, S. Liu, Z. Lu, C. Lu, X. Leng, Y. Lan and Q. Shen, $C(sp^3)$-CF_3 Reductive elimination from a five-coordinate neutral copper(III) complex, *J. Am. Chem. Soc.*, 2020, **142**, 9785; (*d*) Y. Xiong, Z. Du, H. Chen, Z. Yang, Q. Tan, C. Zhang, L. Zhu, Y. Lan and M. Zhang, Well-designed phosphine–urea ligand for highly diastereo- and enantioselective 1,3-dipolar cycloaddition of methacrylonitrile: a combined experimental and theoretical study, *J. Am. Chem. Soc.*, 2019, **141**, 961; (*e*) L. A. López and J. González, Copper(I)-carbenes as key intermediates in the [3 + 2]-cyclization of pyridine derivatives with alkenyldiazoacetates: a computational study, *Org. Biomol. Chem.*, 2019, **17**, 646.

6 M. J. Frisch, G. W. Trucks, H. B. Schlegel, G. E. Scuseria, M. A. Robb, J. R. Cheeseman, G. Scalmani, V. Barone, B. Mennucci, G. A. Petersson, H. Nakatsuji, M. Caricato, X. Li, H. P. Hratchian, A. F. Izmaylov, J. Bloino, G. Zheng, J. L. Sonnenberg, M. Hada, M. Ehara, K. Toyota, R. Fukuda, J. Hasegawa, M. Ishida, T. Nakajima, Y. Honda, O. Kitao, H. Nakai, T. Vreven, J. A. Montgomery Jr., J. E. Peralta, F. Ogliaro, M. Bearpark, J. J. Heyd, E. Brothers, K. N. Kudin, V. N. Staroverov, R. Kobayashi, J. Normand, K. Raghavachari, A. Rendell, J. C. Burant, S. S. Iyengar, J. Tomasi, M. Cossi, N. Rega, J. M. Millam, M. Klene, J. E. Knox, J. B. Cross, V. Bakken, C. Adamo, J. Jaramillo, R. Gomperts, R. E. Stratmann, O. Yazyev, A. J. Austin, R. Cammi, C. Pomelli, J. W. Ochterski, R. L. Martin, K. Morokuma, V. G. Zakrzewski, G. A. Voth, P. Salvador, J. J. Dannenberg, S. Dapprich, A. D. Daniels, O. Farkas, J. B. Foresman, J. V. Ortiz, J. Cioslowski and D. J. Fox, *Gaussian 09, Revision A.02*, Gaussian, Inc., Wallingford CT, 2009.

7 (*a*) Y. Zhao and D. G. Truhlar, Density functionals with broad applicability in chemistry, *Acc. Chem. Res.*, 2008, **41**, 157; (*b*) Y. Zhao and D. G. Truhlar, The M06 suite of density functionals for main group thermochemistry, thermochemical kinetics, noncovalent interactions, excited

states, and transition elements: two new functionals and systematic testing of four M06-class functionals and 12 other functionals, *Theor. Chem. Acc.*, 2008, **120**, 215.

8 (*a*) K. Fukui, The Path of chemical reactions - the IRC approach, *Acc. Chem. Res.*, 1981, **14**, 363; (*b*) T. H. Dunning Jr. and P. J. Hay, in *Modern Theoretical Chemistry*, ed. H. F. Schaefer III, Plenum Press, New York, 1977, pp. 1–28.

9 P. Schwerdtfeger, The pseudopotential approximation in electronic structure theory, *ChemPhysChem*, 2011, **12**, 3143.

10 (*a*) P. J. Hay and W. R. Wadt, *Ab initio effective* core potentials for molecular calculations. Potentials for the transition metal atoms Sc to Hg, *J. Chem. Phys.*, 1985, **82**, 270; (*b*) W. R. Wadt and P. J. Hay, *Ab initio effective* core potentials for molecular calculations. Potentials for main group elements Na to Bi, *J. Chem. Phys.*, 1985, **82**, 284; (*c*) P. J. Hay and W. R. Wadt, Ab initio effective core potentials for molecular calculations. Potentials for K to Au including the outermost core orbitals, *J. Chem. Phys.*, 1985, **82**, 299.

11 (*a*) K. Fukui, Formulation of the reaction coordinate, *J. Phys. Chem.*, 1970, **74**, 4161; (*b*) C. Gonzalez and H. B. Schlegel, An improved algorithm for reaction path following, *J. Chem. Phys.*, 1989, **90**, 2154; (*c*) C. Gonzalez and H. B. Schlegel, Reaction path following in mass-weighted internal coordinates, *J. Phys. Chem.*, 1990, **94**, 5523.

12 D. Andrae, U. Häußermann, M. Dolg, H. Stoll and H. Preuß, Energy-adjusted *ab initio* pseudopotentials for the second and third row transition elements, *Theor. Chim. Acta*, 1990, **77**, 123.

13 A. V. Marenich, C. J. Cramer and D. G. Truhlar, Universal solvation model based on solute electron density and on a continuum model of the solvent defined by the bulk dielectric constant and atomic surface tensions, *J. Phys. Chem. B*, 2009, **113**, 6378.

14 For selected examples of DFT calculations demonstrating the proton transfer assisted by water or an anion, see: (*a*) F.-Q. Shi, X. Li, Y. Xia, L. Zhang and Z.-X. Yu, DFT study of the mechanisms of in water Au(I)-catalyzed tandem [3,3]-rearrangement/Nazarov reaction/[1,2]-hydrogen shift of enynyl acetates: a proton-transport catalysis strategy in the water-catalyzed [1,2]-hydrogen shift, *J. Am. Chem. Soc.*, 2007, **129**, 15503; (*b*) A. Rossin, L. Gonsalvi, A. D. Phillips, O. Maresca, A. Lledós and M. Peruzzini, Water-assisted H-H bond splitting mediated by $[CpRu(PTA)_2Cl]$ (PTA = 1,3,5-triaza-7-phosphaadamantane). A DFT analysis, *Organometallics*, 2007, **26**, 3289; (*c*) Y. Xia, Y. Liang, Y. Chen, M. Wang, L. Jiao, F. Huang, S. Liu, Y. Li and Z.-X. Yu, An unexpected role of a trace amount of water in catalyzing proton transfer in phosphine-catalyzed (3 + 2) cycloaddition of allenoates and alkenes, *J. Am. Chem. Soc.*, 2007, **129**, 3470; (*d*) Y. Xia, A. S. Dudnik, Y. Li and V. Gevorgyan, On the validity of Au-vinylidenes in the gold-catalyzed 1,2-migratory cycloisomerization of skipped propargylpyridines, *Org. Lett.*, 2010, **12**, 5538; (*e*) Y. Qiu, C. Fu, X. Zhang and S. Ma, Studies on $[PtCl_2]$- or [AuCl]-catalyzed cyclization of 1-(Indol-2-yl)-2,3-allenols: The effects of water/steric hindrance and 1,2-migration selectivity, *Chem. – Eur. J.*, 2014, **20**, 10314.

15 For all results of the 1-octyne participated system, see the ESI.†